INTERNATIONAL JOURNAL FOR NUMERICAL METHODS IN ENGINEERING, VOL. 29, 1639–1652 (1990)

EFFECT OF INTEGRATION METHODS ON THE SOLUTION OF AN ADIABATIC SHEAR BANDING PROBLEM

R. C. BATRA AND C. H. KIM

Department of Mechanical and Aerospace Engineering and Engineering Mechanics, University of Missouri-Rolla, Rolla, MO 65401–0249, U.S.A.

SUMMARY

Equations governing the thermomechanical deformations of a block made of a viscoplastic material, and undergoing overall simple shearing deformations, are stiff in the sense that time scales associated with the heat conduction, viscous effects, strain hardening and strain-rate hardening may differ by several orders of magnitude as localization of the deformation initiates and proceeds. Because of the presence of high spatial gradients within the region of localization of the deformation, we also consider a viscoplasticity theory in which the strain gradient is taken as a kinematic variable. The Galerkin approximation of the pertinent initial-boundary-value problem yields an initial-value problem involving a set of coupled non-linear ordinary differential equations. The solution of these equations by the Crank–Nicolson, Adams–Moulton and the Gear methods reveals that the three methods give qualitatively similar results. However, quantitatively the results by the three methods differ somewhat, the difference being more for the dipolar theory.

INTRODUCTION

Adiabatic shear banding refers to the localization of deformation into a narrow band of intense straining that occurs during high rate plastic deformation such as machining, explosive forming and ballistic penetration. Practical interest in the phenomenon derives from the fact that once a shear band has formed, subsequent deformations of the body are concentrated within these narrow regions with the rest of the body not deforming at all. Thus, shear bands act as precursors to shear fracture.

Since the time Zener and Hollomon[1] observed these shear bands in a steel plate punched by a standard die, there have been numerous analytical,[2–9] experimental[6–9] and numerical studies[10–14] aimed at delineating factors that enhance or inhibit the initiation and subsequent growth of shear bands. Numerical computations of Wright and Walter[12] reveal that the shear stress collapses as the shear band begins to grow, and those of Batra and Kim[13] indicate that, as the shear stress drops rapidly, an unloading elastic shear wave emanates outwards from the severely deforming region.

The aforementioned numerical works and experimental observations[7] indicate that the peak strain gradients reach 0·2 per μm or higher within the shear band. It, therefore, seems reasonable to include the strain gradient as an independent kinematic variable. Dillon and Kratochvil[15] have suggested that one way to account for the interaction among dislocations is to include strain gradients and dipolar stresses in equations governing the plastic deformations of a body. Wright and Batra,[16] Batra[14] and Batra and Kim[13] have considered these dipolar effects. Their numerical solutions of the dynamic thermomechanical problem show that dipolar effects delay the initiation

0029–5981/90/081639–14$07.00

Received 30 June 1989
Revised 5 November 1989

of shear bands and retard their growth compared to simple materials. Coleman and Hodgdon[17] and Zbib and Aifantis[18] have studied quasistatic deformations of rigid perfectly plastic materials and assumed that the yield stress in shear depends upon higher order gradients of the shear strain. Consideration of these non-local constitutive relations[14–18] introduces an additional length scale that is characteristic of the material. For rate-dependent heat conducting solids, other length scales are introduced by viscous and thermal effects. Previous investigations[19] seem to suggest that the length scale associated with non-local effects plays a dominant role in determining the final width of the band. Batra and Kim[20] recently found that the predictions from the dipolar theory based on the Litonski law as modified by Wright and Batra[16] are in closer agreement with the experimental observations of Marchand and Duffy[9] than those of other flow rules not incorporating the dipolar effects.

As has been vividly shown by Needleman,[21] computed results for problems involving the localization of deformation show strong dependence upon the mesh used. In dynamic problems, the numerical technique used to integrate the governing equations also influences the results significantly. Here we report our experience with Gear's stiff method,[22] the Adams–Moulton method[23] and the Crank–Nicolson method[24] for solving the adiabatic shear banding problem for non-polar and dipolar materials. The results obtained by using the three methods on the same spatial mesh differed very little until the deformation began to localize. Once localization occurred, the deformations within the shear band were obtained more accurately by using Gear's method. The time step size needed to compute stable results with the desired accuracy was different for each method.

FORMULATION OF THE PROBLEM

We study the simple shearing deformations of an isotropic, viscoplastic and homogeneous block of material that exhibits strain and strain-rate hardening and thermal softening. In terms of non-dimensional variables the governing equations are

$$\rho\dot{v} = (s - l\sigma_{,y})_{,y}, \quad -1 < y < 1 \tag{1}$$

$$\dot{\theta} = k\theta_{,yy} + s\dot{\gamma}_{\text{p}} + \sigma\dot{d}_{\text{p}}, \quad -1 < y < 1 \tag{2}$$

supplemented by the constitutive relations

$$\dot{s} = \mu(v_{,y} - \dot{\gamma}_{\text{p}}) \tag{3}$$

$$\dot{\sigma} = \mu l(v_{,yy} - \dot{d}_{\text{p}}) \tag{4}$$

$$\dot{\psi} = (s\dot{\gamma}_{\text{p}} + \sigma\dot{d}_{\text{p}}) \Big/ \left(1 + \frac{\psi}{\psi_0}\right)^n \tag{5}$$

$$\dot{\gamma}_{\text{p}} = \Lambda s, \quad \dot{d}_{\text{p}} = \Lambda\sigma \tag{6}$$

and

$$\Lambda = 0 \quad \text{if} \quad \tau \leqslant \left(1 + \frac{\psi}{\psi_0}\right)^n (1 - \alpha\theta) \tag{7}$$

otherwise

$$\Lambda = \left[\left\{\tau \Big/ \left(1 + \frac{\psi}{\psi_0}\right)^n (1 - \alpha\theta)\right\}^{1/m} - 1\right] \Big/ b\tau \tag{8}$$

where

$$\tau^2 = s^2 + \sigma^2 \tag{9}$$

Equations (1) and (2) express, respectively, the balance of linear momentum and the balance of internal energy. Here ρ is the mass density, v the x-velocity of a material particle, s the shear stress, σ the dipolar stress associated with the strain gradient, a superimposed dot indicates the material time derivative, a comma followed by y signifies the partial derivative with respect to y, θ is the temperature change from that in the reference configuration, k is the thermal diffusivity, $\dot{\gamma}_p$ is the plastic part of the strain-rate, and $\dot{d}_p$ is the plastic part of the strain-rate gradient. The constitutive relations (3) and (4) are essentially Hooke's law written in terms of rates wherein μ is the shear modulus and l a material characteristic length. We note that $l = 0$ for non-polar materials and is positive for dipolar materials. The work hardening parameter ψ has a rate of evolution that is a function of the rate of plastic work done and describes the work hardening of the material. By following an argument advanced by Green *et al.*,[25] Wright and Batra[16] derived equations (6) for the plastic part of the strain-rate and its gradient. Equation (7) implies that the plastic strain-rate and the plastic strain-rate gradient vanish whenever the effective stress τ is inside or on the loading surface,

$$\tau = \left(1 + \frac{\psi}{\psi_0}\right)^n (1 - \alpha\theta) \tag{10}$$

and Λ is positive whenever the effective stress lies outside the loading surface defined by (10). The foregoing is one version of the viscoplasticity theory; some other constitutive relations proposed for $\dot{\gamma}_p$ have been summarized by Batra and Kim.[20] Substitution for $\dot{\gamma}_p$ and $\dot{d}_p$ from (6) into equations (2)–(4) gives five evolution equations for the five unknowns v, θ, s, σ and ψ.

For the boundary conditions, we take

$$v(\pm 1, t) = \pm 1, \quad \theta_{,y}(\pm 1, t) = 0, \quad \sigma(\pm 1, t) = 0 \tag{11}$$

That is, the body is placed in a perfectly insulated hard loading device in the sense that the velocity is prescribed at the top and bottom surfaces. Also, the dipolar stress is presumed to be zero at the top and bottom surfaces. The boundary conditions for σ are needed because of the term $\sigma_{,yy}$ in equation (1). For homogeneous simple shearing deformations of the body, $\dot{d} \equiv v_{,yy} = 0$, and hence σ vanishes throughout the body. Since we are interested in studying the localization of the deformation and have assumed the body to be homogeneous, we must give non-uniform initial conditions. Accordingly we take

$$\begin{gathered} \theta(y, 0) = 0{\cdot}1(1 - y^2)^9 \, e^{-5y^2}, \quad v(y, 0) = y \\ \sigma(y, 0) = 0, \quad s(y, 0) = 1{\cdot}0, \quad \psi(y, 0) = 0 \end{gathered} \tag{12}$$

That is, the transient effects are presumed to have died out, the shear stress everywhere equals the yield stress in a quasistatic, isothermal simple shear test on the material of the block and the body is given a temperature perturbation symmetric around the centre line $y = 0$. Both the amplitude and the width of the temperature perturbation affect the time of initiation of the localization of the deformation. The temperature perturbation models a material inhomogeneity or flaw in the body and the amplitude 0·1 of the perturbation represents, in some sense, the strength of the defect.

FINITE ELEMENT FORMULATION OF THE PROBLEM

As we have done in the past,[13,14] we obtain a semidiscrete formulation, by using the Galerkin method (e.g. see Hughes[26]), of the balance laws (1) and (2) and the constitutive relations (3) to (5).

We note that $\dot{\gamma}_p$ and $\dot{d}_p$ can be eliminated by using equations (6). The result is a system of coupled non-linear ordinary differential equations

$$\dot{\mathbf{u}} = \mathbf{f}(\mathbf{u}, \psi_0, \mu, m, n, \alpha, b) \tag{13}$$

Here $\mathbf{u}$ is a vector of nodal values of the velocity, temperature, shear stress, dipolar stress and the work hardening parameter. The total number of unknowns or the number of components of $\mathbf{u}$ equals five times the number of nodes. The vector valued function $\mathbf{f}$ is a non-linear function of $\mathbf{u}$ and of the material parameters μ, ψ_0, m, n, α and b. From the initial conditions (12) one can deduce the initial conditions on $\mathbf{u}$. Batra and Wright[27] have demonstrated that the integration of these equations by the Crank–Nicolson method and the forward difference method gives virtually identical results for non-polar materials for which $l = 0$ and slightly different results for dipolar materials with $l = 0{\cdot}01$ and applied strain-rate $\dot{\gamma}_0 = 1000\ \mathrm{s}^{-1}$. Here we solve these equations by using the:

(i) Crank–Nicolson method;[24]
(ii) Adams-Moulton method;[23] and
(iii) Gear stiff method.[22]

For the first two methods, the time increment Δt is kept fixed, and for the Gear method, the IMSL subroutine LSODE adjusts it adaptively till a solution of the non-linear equations (13) can be computed to the prescribed degree of accuracy. Of the three methods, the Gear method has been found to be the most efficient one as far as the CPU time required to integrate these equations is concerned.

COMPUTATION AND DISCUSSION OF RESULTS

In order to compute numerical results, we took the following values of various material parameters:

$$\begin{gathered} m = 0{\cdot}025, \quad n = 0{\cdot}07, \quad b = 5 \times 10^7, \quad \alpha = 0{\cdot}358 \\ \mu = 240{\cdot}24, \quad \rho = 3{\cdot}928 \times 10^{-3}, \quad k = 3{\cdot}978 \times 10^{-4}, \quad \psi_0 = 0{\cdot}017 \end{gathered} \tag{14}$$

Except for the value of α, values of other parameters are for a typical hard steel, $\dot{\gamma}_0 = 5000\ \mathrm{s}^{-1}$ and the height of the block = 5·16 mm. The presumed value of α equals nearly five times the actual value and implies that the material melts at $\theta = 2{\cdot}793$. This rather large value of α should enhance the initiation and possibly subsequent development of the shear band. However, the precise values of various parameters should not affect the relative performance of the different integration schemes.

For non-polar materials (i.e. $l = 0{\cdot}0$), it is reasonable to assume

$$v(-y, t) = -v(y, t),\ \theta(-y, t) = \theta(y, t),\ s(-y, t) = s(y, t),\ \psi(-y, t) = \psi(y, t) \tag{15}$$

and hence reduce the problem to the one for the domain [0, 1]. For dipolar materials (i.e. $l > 0{\cdot}0$), Batra[28] has shown that $\sigma(y, t)$ is antisymmetric with respect to y, $\sigma(-y, t) = -\sigma(y, t)$. Loosely speaking, the antisymmetry of σ follows from its affine dependence upon $v_{,yy}$ and v satisfies $(15)_1$. It follows that $\sigma(0, t) = 0$, while the field variables v, θ, s and ψ satisfy (15). Thus, the problem for both non-polar and dipolar materials can be solved over the domain [0, 1] and the boundary conditions (11) replaced by

$$\begin{gathered} v(0, t) = 0, \quad \theta_{,y}(0, t) = 0, \quad \sigma(0, t) = 0 \\ v(1, t) = 1, \quad \theta_{,y}(1, t) = 0, \quad \sigma(1, t) = 0 \end{gathered} \tag{16}$$

Results presented below are for a fixed non-uniform finite element mesh with 100 linear elements. The y-co-ordinate of nodal points is given by

$$y_n = \left(\frac{n-1}{100}\right)^3, \quad n = 1, 2, \ldots, 101 \tag{17}$$

Thus, the mesh used is very fine near the centre of the block where significant deformations are expected to occur. For Crank–Nicolson and Adams–Moulton methods fixed $\Delta t = 5 \times 10^{-6}$ was used, but for the Gear stiff method the size of the time step is adjusted adaptively in the subroutine LSODE.

Results for Non-polar materials ($l = 0{\cdot}0$)

Figure 1 depicts the evolution of the plastic strain-rate, the temperature and the shear stress at the centre of the block as computed by the three methods. In order to magnify any differences, the results are plotted for portions of the problem's time span. The results computed by the three methods agree with each other qualitatively. The results obtained by using the Crank–Nicolson method and the Adams–Moulton method agree with each other but are delayed as compared to the results obtained by using Gear's stiff method. A reason for this seems to be that the Gear method gives a slightly higher temperature at the centre as compared to that computed with the other two methods. Plastic straining produces heating which, by raising temperature, has a softening effect that promotes a higher plastic strain-rate. This may cause an instability, the localization of plastic deformation. We note that the convergence criterion, used for the Crank–Nicolson and the Adams–Moulton methods, was the same but that used in the IMSL subroutine LSODE, based on the Gear method, could be different. In the former case, the solution of algebraic equations obtained from (13) was assumed to have converged if at each node point

$$\left|\frac{\Delta v}{v}\right| + \left|\frac{\Delta s}{s}\right| + \left|\frac{\Delta \theta}{\theta}\right| + \left|\frac{\Delta \psi}{\psi}\right| + \left|\Delta \sigma\right| \leqslant 0{\cdot}001 \tag{18}$$

and with the Gear method, absolute and relative tolerances were prescribed to be 0·0001 and 0·0001 respectively. We note that the Crank–Nicolson and the Adams–Moulton methods become unstable soon after the deformation localizes.

Figure 2 shows how the shear stress, work hardening parameter, plastic strain-rate and temperature evolve in the block as computed by the Gear method. The shear stress stays uniform throughout the block. It initially rises because of the hardening of the material due to plastic working and strain-rate effects. The temperature increases slowly owing to the heat generated because of plastic working and the assumption of insulated boundaries. When the softening caused by the heating of the material overcomes the hardening due to plastic strain and plastic strain-rate effects, the shear stress begins to drop. Subsequently the deformation begins to localize and the temperature at points near the centre of the block rises sharply, accompanied by a steep drop in the shear stress. The plots of the plastic strain-rate, temperature rise and the work hardening parameter in Figure 2 show the severely deforming region is progressively getting narrower. The waviness in the spatial variation of the shear stress and the work hardening parameter suggests that calculations have started to become unstable, and they were discontinued.

Figure 3 depicts the differences in the spatial variation of the plastic strain-rate, the temperature and the shear stress as computed by the three methods. In each case, the results are plotted for the solution just before it becomes unstable. For the plot of the plastic strain-rate, the spatial

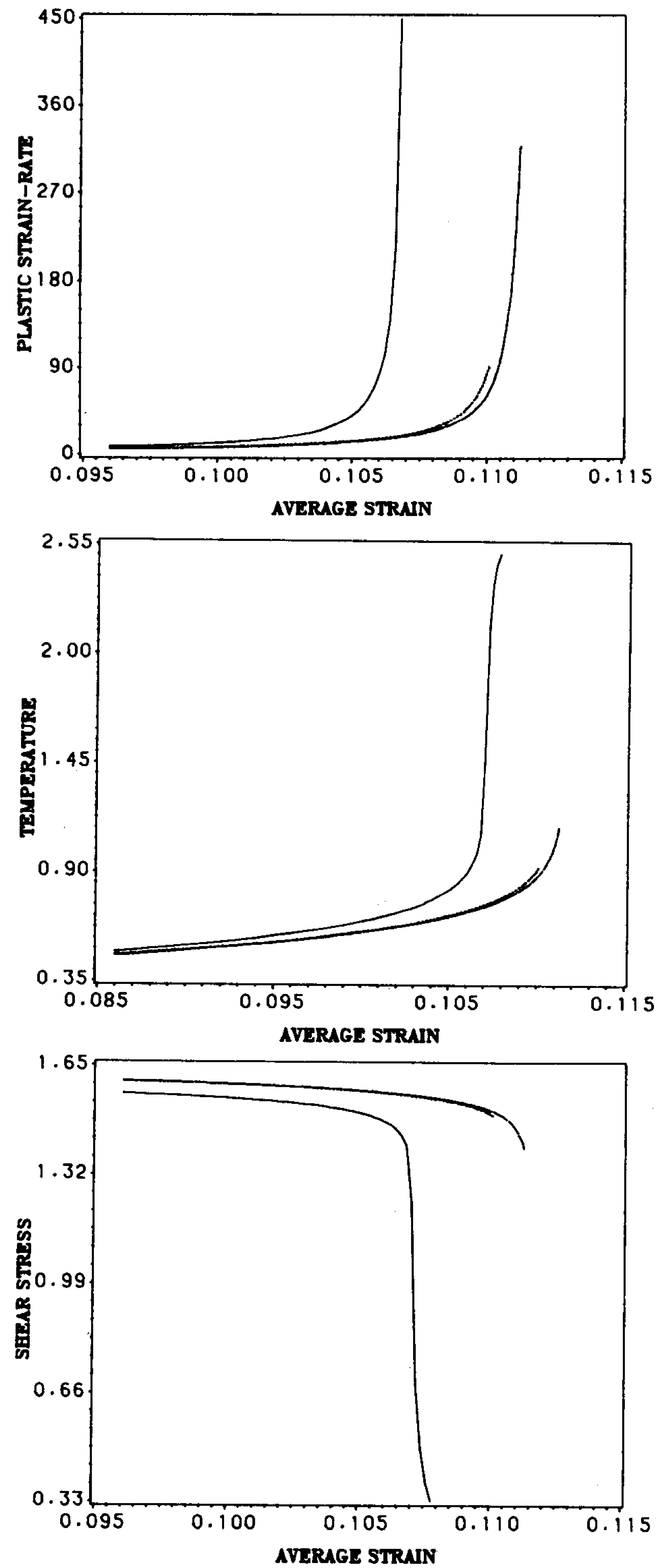

Figure 1. A comparison of the evolution of the plastic strain-rate, temperature and the shear stress at the centre of the specimen for non-polar materials (—— Gear's method, — — — Adams–Moulton method, -- -- -- -- Crank–Nicolson method)

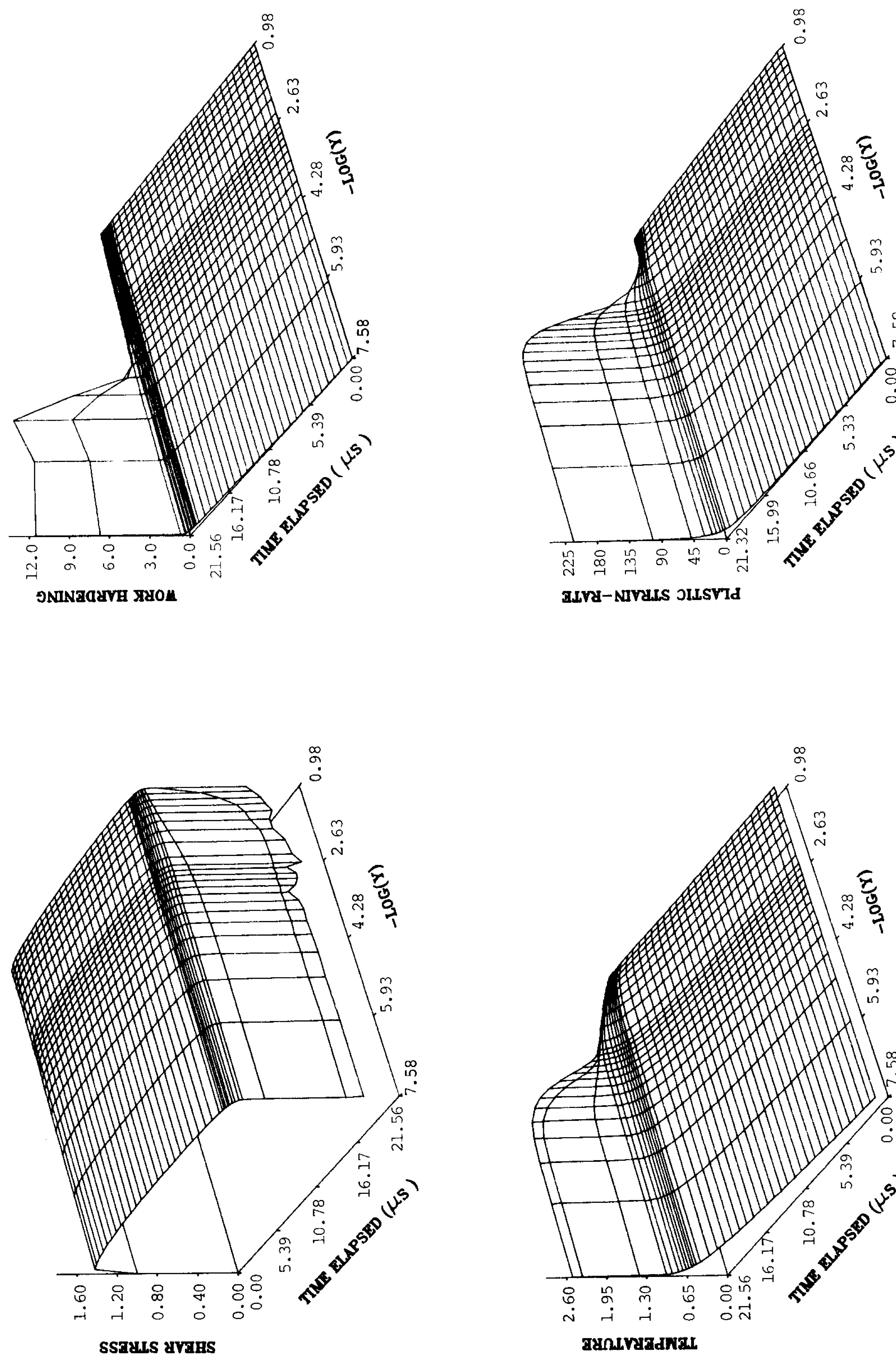

Figure 2. Spatial and temporal variation of the plastic strain-rate, temperature, shear stress and the work hardening parameter for non-polar materials as computed by the Gear method

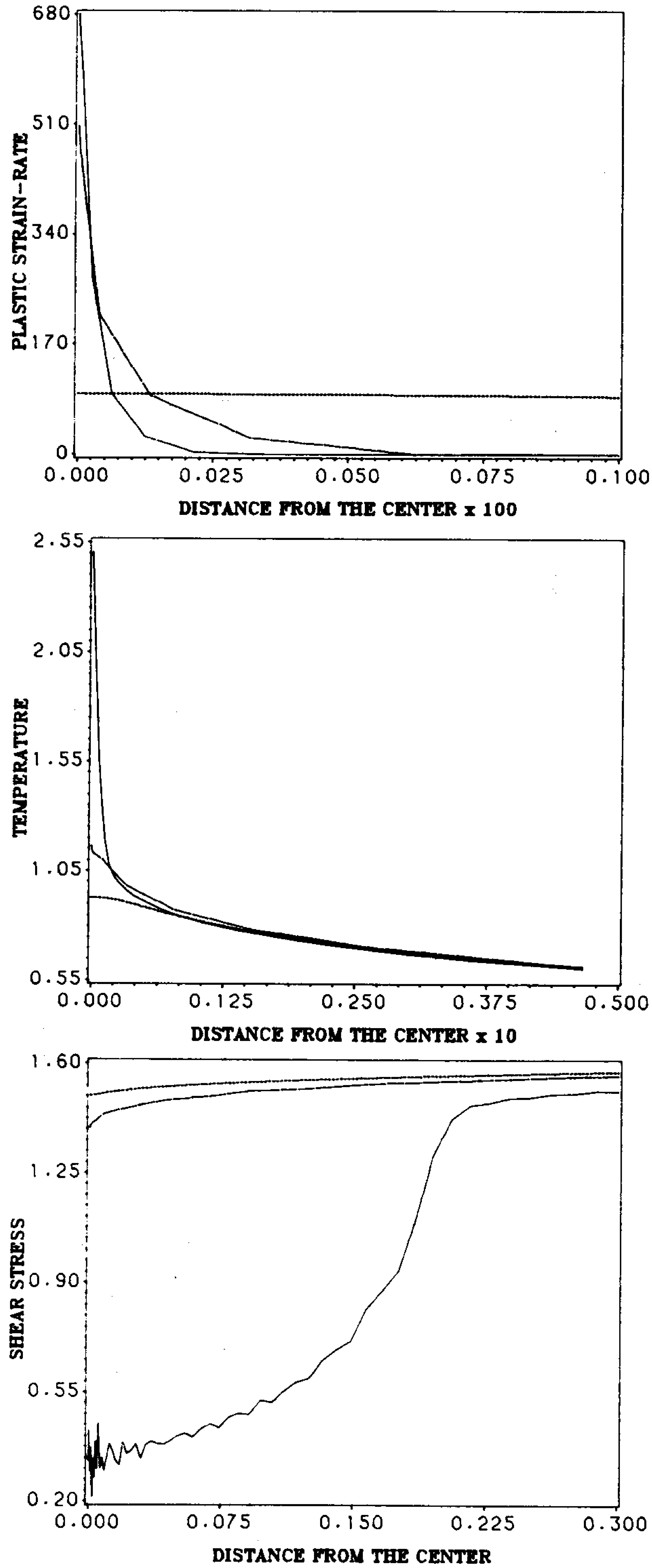

Figure 3. A comparison of the spatial variation of the shear stress, temperature and plastic strain-rate within the region of localization of the deformation for non-polar materials (—— Gear's method, — — — — Adams–Moulton method, -- -- -- -- Crank–Nicolson method)

distance covered is very small in order to show the area where localization of deformation occurs. If one were to plot the spatial variation of the plastic strain-rate as computed by the Crank–Nicolson method, the width of the severely deformed region would be considerably larger than that obtained with the other two methods. This is mainly due to the fact that the solution becomes unstable soon after the deformation begins to localize. During the growth of the shear band, the width of the severely deforming region decreases rapidly. This also explains the difference between the results computed with the Gear and the Adams–Moulton methods. However, the three methods seem to give qualitatively similar results.

Results for dipolar materials ($l = 0{\cdot}005$)

The evolution of the plastic strain-rate, the temperature and the shear stress at the centre of the specimen as computed by the three methods is plotted in Figure 4. Unlike for non-polar materials, the Adams–Moulton method gives slightly higher values of the temperature than the other two methods. The temperature computed by the Gear method is between the values found by using the other two methods. However, the Gear method gives values of the shear stress which are lower than those given by the other two methods except when they start to drop. Then the Gear method and the Adams–Moulton method give virtually identical values of the shear stress. As with non-polar materials, the Crank–Nicolson method becomes unstable first, during the time the shear band is growing. We note that the gradients of the strain-rate act as a stabilizing factor.

A comparison of these results with those in Figure 1 establishes the previously[13] noted result that the consideration of dipolar effects delays the initiation and the rate of growth of the adiabatic shear band. The latter follows from the fact that the rate of rise of the plastic strain-rate subsequent to the initiation of the localization of the deformation is less for dipolar materials as than that for non-polar materials. Both the delay in the initiation and development of the shear band depend upon the value of the material characteristic length l. Figure 5 shows the variation of the temperature, shear stress, dipolar stress and the plastic strain-rate within the specimen at different values of time as computed by the Gear method. Until the time the deformation begins to localize, the shear stress stays uniform throughout the specimen. When the localization of the deformation is in progress the shear stress drops gradually. It first stays uniform throughout the specimen but soon becomes non-uniform, with the smallest value occurring at a slight distance from the centre. At the same time the dipolar stress σ, which equalled zero until the shear stress started becoming non-uniform, begins to increase in magnitude. Its highest value occurs close to the point where the shear stress takes on the smallest value. Note that $(s - l\sigma_{,y})$ acts as a flux for the linear momentum and, as pointed out in Reference 13, it decreases gradually, remains uniform with respect to y and is positive even when s is negative. It is the effective stress τ rather than s or σ that determines whether a material point is deforming plastically or not, and in the former case determines the plastic strain-rate. The plots of the plastic strain-rate and the temperature in Figure 5 reveal the gradual decrease in the thickness of the severely deforming region. The temperature and the plastic strain-rate at points near the centre of the specimen rise sharply at the initiation of the localization of the deformation. Their rate of rise is less than that of non-polar materials. When the shear stress has dropped to nearly zero value, the rate of temperature increase slows down but that of plastic strain-rate goes up significantly. The maximum temperature equalled 99·5 per cent of the presumed melting temperature of the material. The shear bands for dipolar materials are wider than those for non-polar materials.

Figure 6 shows the spatial variation of the plastic strain-rate, the temperature and the shear stress as computed by the three methods. The values of the nominal strain γ_{avg} at which these curves are plotted are not the same for the three methods. The three methods give qualitatively

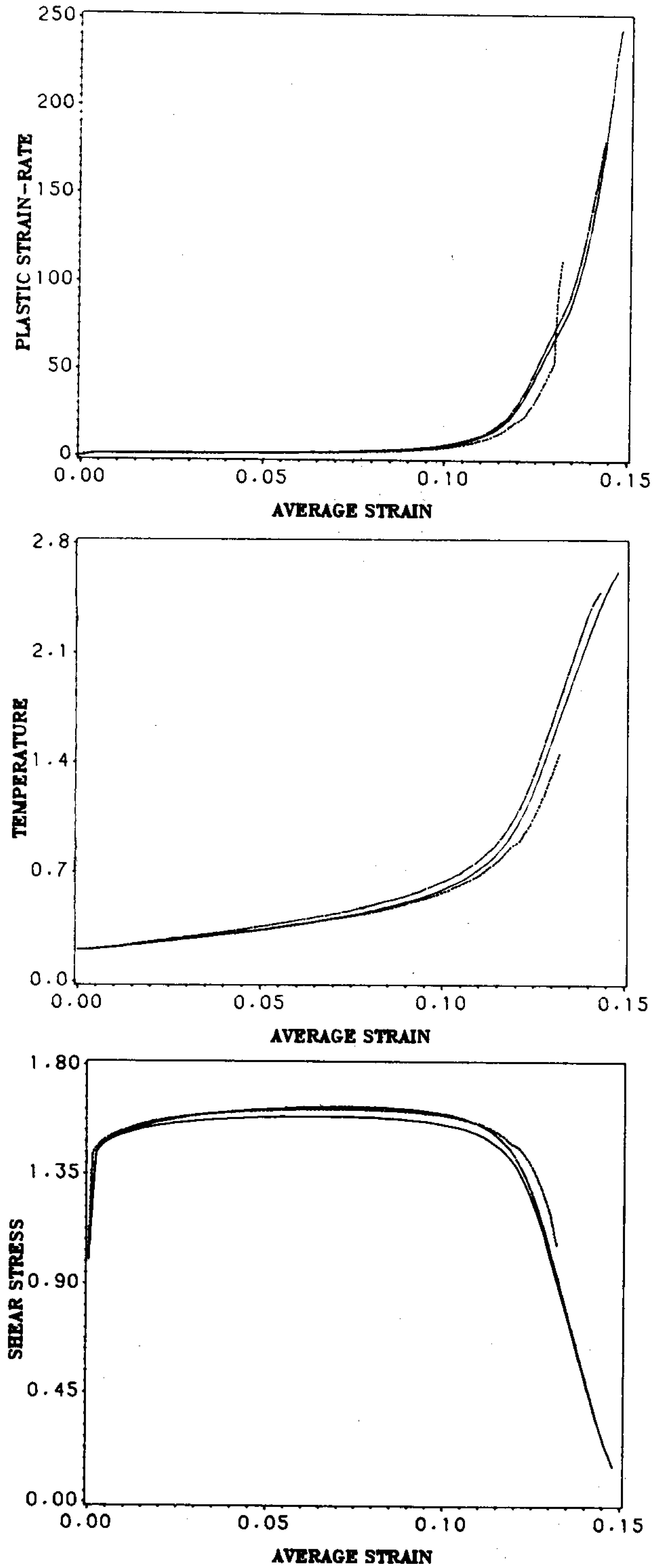

Figure 4. A comparison of the evolution of the plastic strain-rate, temperature and the shear stress at the centre of the specimen for dipolar materials with $l = 0{\cdot}005$ (—— Gears method, — — — — — Adams–Moulton method, -- -- -- -- Crank–Nicolson method)

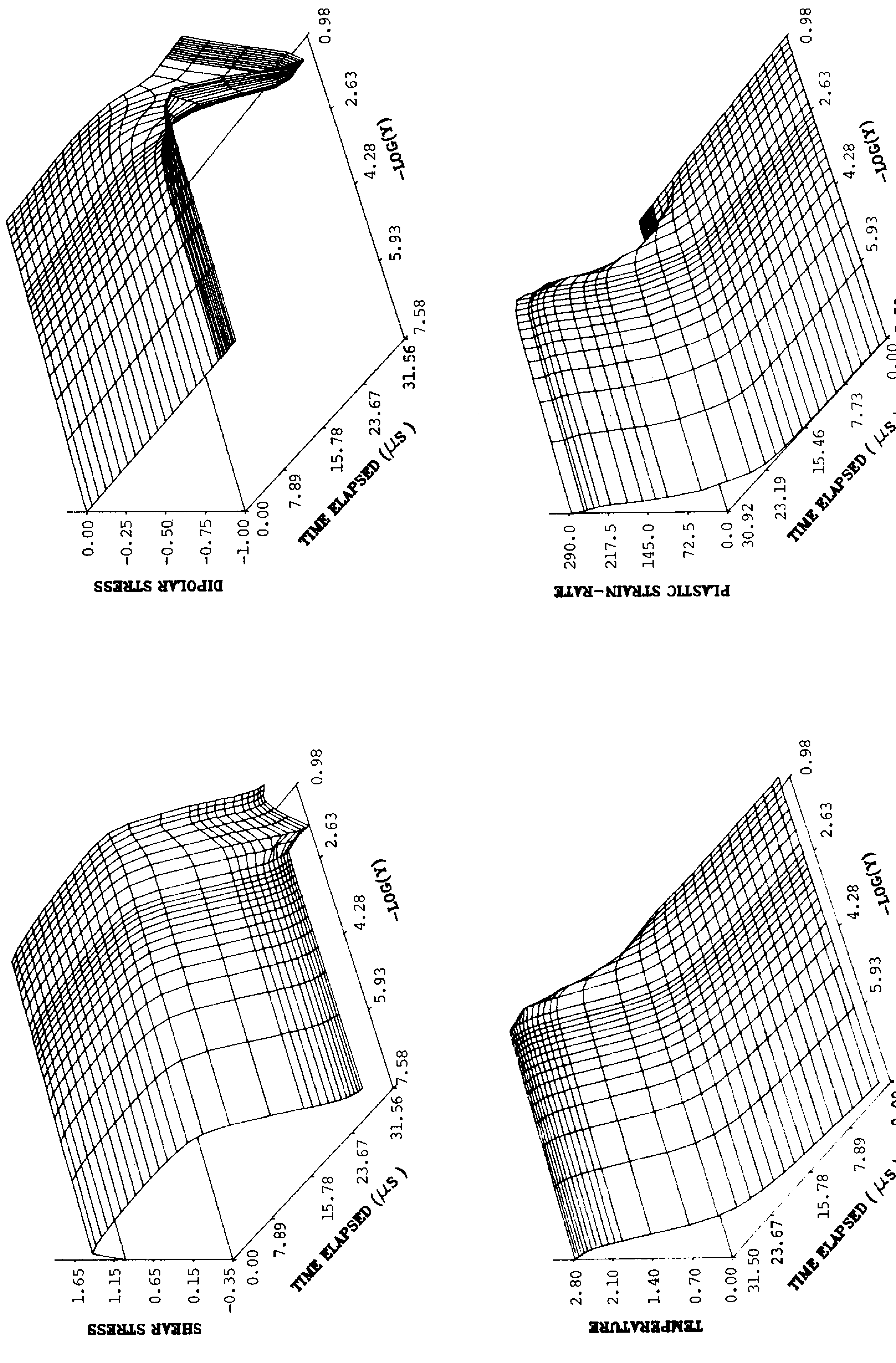

Figure 5. Spatial and temporal variation of the plastic strain-rate, temperature, shear stress and the dipolar stress for dipolar materials with $l = 0{\cdot}005$ as computed by the Gear method

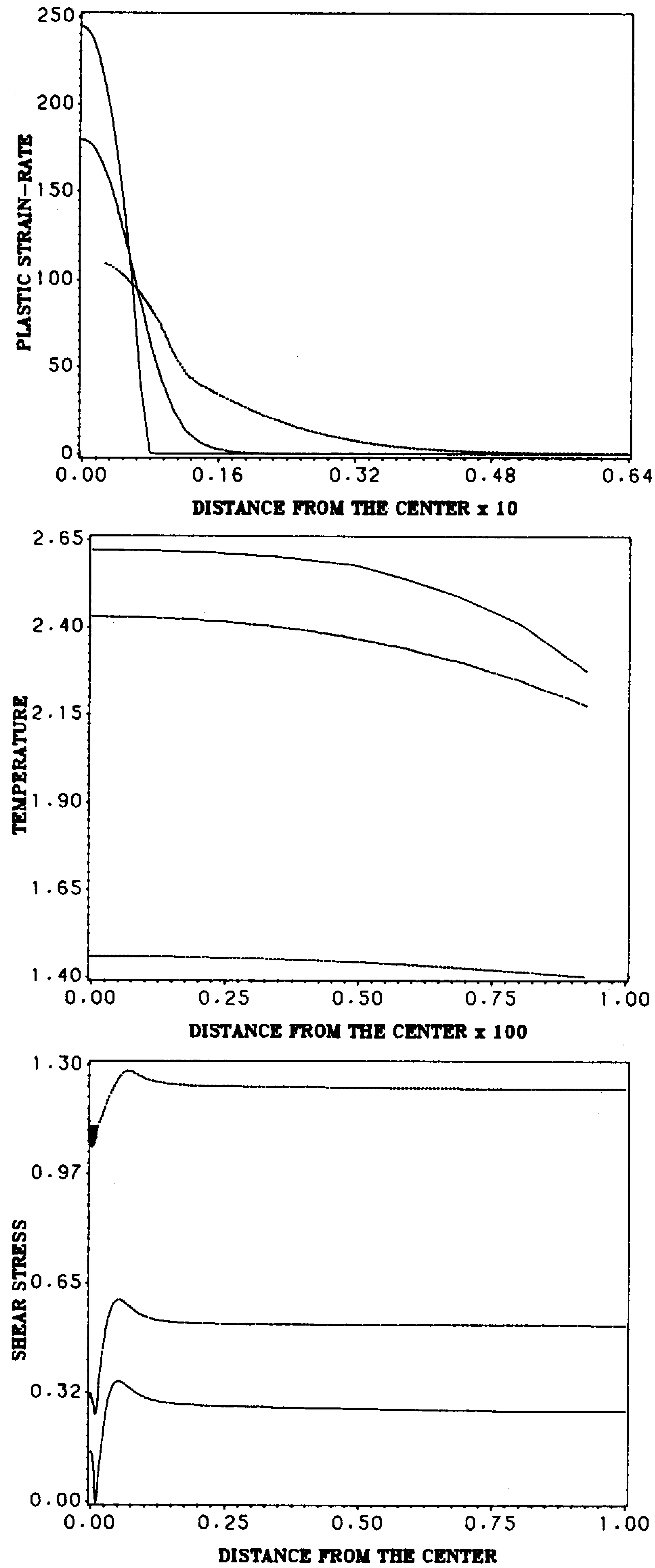

Figure 6. A comparison of the spatial variation of the plastic strain-rate, temperature and shear stress within the region of localization of the deformation for dipolar materials with $l = 0{\cdot}005$ (—— Gear's method, — — — — — Adams–Moulton method, --- --- --- --- Crank–Nicolson method)

similar results. The computations with the Gear method were stopped when the shear stress s at any point became zero. The computations remain stable and could be carried further if desired.

CONCLUSIONS

For both non-polar and dipolar materials, the three methods give qualitatively similar results. However, they exhibit different delay characteristics as far as the evolution of the field variables at the centre of the specimen is concerned. For non-polar materials, the Crank–Nicolson and the Adams–Moulton methods delay the initiation of the localization process, defined as the instant when the rate of increase of the plastic strain-rate is extremely high. The Gear method gave stable results while the other two methods became unstable soon after the deformations began to localize. For dipolar materials with $l = 0{\cdot}005$, the initiation of the shear band with the Gear method was delayed slightly compared to the results using the Adams–Moulton method, and the Crank–Nicolson method caused the band to initiate at an even larger value of γ_{avg}. The Adams–Moulton and the Crank–Nicolson methods gave stable results even when the localization of the deformation was in progress, but became unstable prior to the time when the shear stress at any point became zero or negative. Results obtained with the Gear method remained stable throughout the development of the shear band.

ACKNOWLEDGEMENTS

This work was supported by the U.S. National Science Foundation Grant MSM–8715952 and the U.S. Army Research Office Contract DAAL03–88–K–0184 to the University of Missouri-Rolla. We are grateful to the IBM Corporation for giving us the CPU time on its 3090 machine under the RSP1049. We are indebted to an anonymous referee for the detailed comments that helped improve the presentation of the work.

REFERENCES

1. C. Zener and J. H. Hollomon, 'Effect of strain-rate on plastic flow of steel', *J. Appl. Phys.*, **14,** 22–32 (1944).
2. R. J. Clifton, J. Duffy, K. A. Hartley and T. G. Shawki, 'On critical conditions for shear band formation at high strain rates', *Scripta Metall.*, **18,** 443–448 (1984).
3. Y. L. Bai, 'A criterion for thermoplastic shear instability', in M. A. Meyers and L. E. Murr (eds.), *Shock Waves and High Strain-Rate Phenomenon in Metals*, Plenum Press, New York, 1981, pp. 277–283.
4. T. J. Burns, 'Approximate linear stability analysis of a model of adiabatic shear band formation', *Q. Appl. Math.*, **43,** 65–74 (1985).
5. L. Anand, K. H. Kim and T. G. Shawki, 'Onset of shear localization in viscoplastic solids', *J. Mech. Phys. Solids*, **35,** 407–429 (1987).
6. U. S. Lindholm and G. R. Johnson, 'Strain-rate effects in metals at large strain-rates', in J. Mescal and V. Weiss (eds.), *Material Behavior Under High Stresses and Ultrahigh Loading Rates*, Plenum Press, New York, 1983, pp. 61–79.
7. G. L. Moss, 'Shear strain, strain rates and temperature changes in adiabatic shear bands', in M. A. Meyers and L. E. Murr (eds.), *Shock Waves and High Strain-Rate Phenomenon in Metals*, Plenum Press, New York, 1981, pp. 299–312.
8. L. S. Costin, E. E. Crisman, R. H. Hawley and J. Duffy, 'On the localization of plastic flow in mild steel tubes under dynamic torsion loading', *Inst. Phys. Conf. Ser.*, **47,** 90–100 (1979).
9. A. Marchand and J. Duffy, 'An experimental study of the formation process of adiabatic shear bands in a structural steel', *J. Mech. Phys. Solids*, **36,** 251–283 (1988).
10. T. W. Wright and R. C. Batra, 'The initiation and growth of adiabatic shear bands', *Int. J. Plasticity*, **1,** 205–212 (1985).
11. A. Needleman, 'Dynamic shear band development in plane strain', *J. Appl. Mech.*, **56,** 1–9 (1989).
12. T. W. Wright and J. Walter, 'On stress collapse in adiabatic shear bands', *J. Mech. Phys. Solids*, **32,** 119–132 (1984).
13. R. C. Batra and C. H. Kim, 'Adiabatic shear banding in elastic–viscoplastic nonpolar and dipolar materials', *Int. J. Plasticity*, **6,** (1990) to appear.
14. R. C. Batra, 'The initiation and growth of, and the interaction among adiabatic shear bands in simple and dipolar materials', *Int. J. Plasticity*, **3,** 75–89 (1987).
15. O. W. Dillon and J. Kratochvil, 'A strain gradient theory of plasticity', *Int. J. Solids Struct.*, **6,** 1513–1533 (1970).
16. T. W. Wright and R. C. Batra, 'Adiabatic shear bands in simple and dipolar plastic materials', in K. Kawata and J.

Shioiri (eds.), *IUTAM Symp. on Macro-and Micro-Mechanics of High Velocity Deformation and Fracture*, Tokyo, Japan, Aug, 12–15, 1985, Springer–Verlag, Berlin, 1987, pp. 189–201.
17. B. D. Coleman and M. L. Hodgdon, 'On shear bands in ductile materials', *Arch. Ratl. Mech. Anal.*, **90,** 219–247 (1985).
18. H. M. Zbib and E. C. Aifantis, 'On the structure and width of shear bands', *Scripta Metall.*, **22,** 703–708 (1988).
19. R. C. Batra and C. H. Kim, 'Effect of material characteristic length on the initiation, growth and band width of adiabatic shear bands in dipolar materials', *J. Physique*, **49,** (C3), 41–46 (1988).
20. R. C. Batra and C. H. Kim, 'Effect of viscoplastic flow rules on the initiation and growth of shear bands at high strain rates', *J. Mech. Phys. Solids* (in press).
21. A. Needleman, 'Material rate dependence and mesh sensitivity in localization problems', *Comp. Methods Appl. Mech. Eng.*, **67,** 69–85 (1988).
22. C. W. Gear, *Numerical Initial Value Problems in Ordinary Differential Equations*, Prentice-Hall, Englewood Cliffs, N.J., 1971.
23. R. L. Burden and J. D. Daires, *Numerical Analysis*, Prindle, Weber and Schmidt, Boston, 1985.
24. G. F. Carey and J. T. Oden, *Finite Elements—Computational Aspects*, Prentice-Hall, Englewood Cliffs, N.J., 1984.
25. A. E. Green, B. C. McInnis and P. M. Naghdi, 'Elastic–plastic continua with simple force dipole', *Int. J. Eng. Sci.*, **6,** 373–394 (1968).
26. T. J. R. Hughes, *The Finite Element Method, Linear Static and Dynamic Finite Element Analysis*, Prentice-Hall, Englewood Cliffs, N.J., 1987.
27. R. C. Batra and T. W. Wright, 'A comparison of solutions of adiabatic shear banding problem by forward difference and Crank–Nicolson methods', *Commun. appl. numer. methods*, **4,** 741–748 (1988).
28. R. C. Batra, unpublished work.